

1 **LGR5 CONTROLS EXTRACELLULAR MATRIX PRODUCTION BY STEM CELLS IN THE**
2 **DEVELOPING INTESTINE**

3 Valeria Fernandez Vallone^{1*}, Morgane Leprovots¹, Romain Gerbier¹, Didac Ribatallada-Soriano¹, Anne
4 Lefort¹, Frédéric Libert¹, Gilbert Vassart¹ and Marie-Isabelle Garcia^{1\$}

5 ¹ Institut de Recherche Interdisciplinaire en Biologie Humaine et Moléculaire (IRIBHM), Faculty of
6 Medicine, Université Libre de Bruxelles ULB, Route de Lennik 808, 1070, Brussels, Belgium.

7

8 **\$ Corresponding author:** Marie-Isabelle Garcia : mgarcia@ulb.ac.be

9 Phone: + 32 2 555 6415; Fax: + 32 2 555 4655

10 *** Current address:** Charité-Universitätsmedizin Berlin BCRT / Institut für Experimentelle
11 Endokrinologie, Campus Virchow Klinikum (Südring 10), Augustenburger Platz 1, D-13353 Berlin
12 Tel. +49-(0)30-450-524162; Fax. +49-(0)30-450-524922

13

14 **Keywords:** Lgr5, stem cells, development, organoids, Rspndins

15 **Running title:** Lgr5 controls the stem cell niche

16 **Word count:** 4, 201 words (references and Materials and methods excluded)

17 **Abstract**

18 The Lgr5 receptor is a marker of intestinal stem cells (ISCs) that regulates Wnt/b-catenin signaling. In
19 this study, phenotype analysis of knockin/knockout Lgr5-eGFP-IRES-Cre and Lgr5-DTReGFP
20 embryos revealed that Lgr5 deficiency during Wnt-mediated cytodifferentiation results in amplification
21 of ISCs and early differentiation into Paneth cells, which can be counteracted by in utero treatment with
22 the Wnt inhibitor LGK974. Conditional ablation of Lgr5 postnatally, but not in adults, altered stem cell
23 fate towards the Paneth lineage. Together, these *in vivo* studies suggest that Lgr5 is part of a feedback
24 loop to adjust the Wnt tone in ISCs. Moreover, transcriptome analyses revealed that fetal ISCs generate
25 their own extracellular matrix components, a property lost in adult ISCs, which adopt a definitive
26 epithelialized phenotype and an inflammatory response signature. Absence of Lgr5 in fetal ISCs resulted
27 in reduced extracellular matrix production and accelerated ISC maturation, indicating that Lgr5
28 regulates the ISC niche. Finally, evidences are provided that Rspordin 2 negatively regulates the pool
29 of ISCs in organoids via Lgr5, revealing a sophisticated regulatory process for Wnt signaling in ISC.

30 INTRODUCTION

31 The adult intestinal epithelium is a specialized tissue involved in nutrients absorption and protection
32 against pathogens or environmental toxic agents. Under homeostatic conditions, within few days, this
33 epithelium undergoes rapid and constant renewal supported by a pool of intestinal stem cells (ISCs),
34 also called Crypt Base Columnar cells, identified by the expression of the Lgr5 receptor [1]. Restricted
35 to the bottom of the crypts of Lieberkühn, ISCs have the capacity to both self-renew and give rise to
36 transit amplifying cells, which differentiate along the villus architecture into all the cell lineages of the
37 epithelium, i. e. absorptive Enterocytes, mucus-producing Goblet cells, hormones-secreting
38 Enteroendocrine cells, Paneth cells generating antimicrobial products and the Type 2 immune response-
39 inducer Tuft cells [2]. Other populations of slowly-cycling or label-retaining reserve stem cells have
40 been identified able to efficiently regenerate the intestinal epithelium upon loss of Lgr5-expressing stem
41 cells; additional evidences have been provided for coexistence and possible mutual interconversion
42 between these two stem cell populations [3-5]. How the definitive crypt-villus architecture is reached in
43 the adult intestinal epithelium and how adult stem cells emerge and establish from the embryonic gut
44 tube deriving from endoderm, these are fundamental questions currently subject of active investigation.
45 By using transgenic mouse lines, evidences have been provided that Cdx2 is a master transcription factor
46 required for intestinal specification before the embryonic stage E14 [6-7]. Thereafter, the intestinal
47 epithelium undergoes a profound remodeling, in part instructed by the underlying mesenchyme, leading
48 to appearance of separate domains constituted by villus and intermingled intervillus regions [8-10].
49 Coherent with a proximal-to-distal wave of cytodifferentiation along the intestine mediated by the
50 Wnt/b-catenin pathway around E14.5, the Wnt/β-catenin target gene Lgr5 becomes upregulated and
51 identifies cells (ISC precursors) restricted to the intervillus regions that grow as adult-type organoids in
52 the *ex vivo* culture system [11-14]. After birth, concomitant with Paneth cell lineage differentiation,
53 intestinal crypts will be formed by invagination of the intervillus regions into the surrounding
54 mesenchyme, bearing in their bottom, the Lgr5-expressing adult ISC [15].
55 Despite general consensus on the function of the Lgr5 receptor as a Wnt/β-catenin signaling modulator
56 in stem cells, how it does so remains still controversial. First of all, *in vitro*, binding of the natural ligands

57 Rspondins to the receptor Lgr5 has been demonstrated to either enhance or inhibit the Wnt pathway
58 depending on the cell type analyzed [16-20]. Secondly, *in vivo*, homozygous *Lgr5-LacZNeo*
59 knockin/knockout embryos deficient for Lgr5, exhibited an overactivated Wnt/b-catenin signaling
60 pathway at birth associated with precocious Paneth cell differentiation, this suggesting a negative
61 regulatory function of Lgr5 on this cascade [21]. However, conditional ablation of the Lgr5 function in
62 adults did not result in significant alteration in Paneth cell differentiation [17]. Moreover, the molecular
63 mechanisms associated with Lgr5 function in ISCs are still debated, does this G-protein-coupled
64 receptor simply control Wnt signaling at the extracellular level by trapping the E3 ubiquitin ligase
65 Znrf3/Rnf43 at the cell membrane or does Lgr5 signal *via* its transmembrane domains and intracellular
66 tail [17,22-23] ?.

67 In the present report, we further investigated the role of the Lgr5 receptor during intestinal development
68 by analyzing the transcriptome of Lgr5-expressing or Lgr5-deficient ISC just after the onset of the Wnt-
69 mediated cytodifferentiation (E16) and in adult homeostatic tissues. We provide evidences that Lgr5
70 controls ISC maturation associated with acquisition of a definitive stable epithelial phenotype, that
71 depends on the capacity of ISCs to generate their own extracellular matrix. In addition, using the *ex vivo*
72 culture system, we demonstrate that the Rspondin 2 ligand negatively regulates the pool of ISCs in
73 organoids via the Lgr5 receptor.

74 **RESULTS**

75 ***In utero* inhibition of Wnt activity counteracts premature Paneth cell differentiation induced by**

76 **Lgr5 deficiency in the intestine**

77 To clarify the molecular function of the Lgr5 ISC stem cell marker in the embryonic intestine, we
78 investigated the potential phenotype of knock-in/knockout (KO) homozygous Lgr5 embryos from the
79 Lgr5-GFP-Cre^{ERT2} and Lgr5-DTReGFP mouse strains [1,24]. Since Lgr5 KOs generated from both
80 transgenic lines showed neonatal lethality associated with ankyloglossia, histological analyses were
81 performed at E18.5. Despite no evidence of gross architectural epithelial alterations, Lgr5 KOs exhibited
82 early differentiation towards the Paneth lineage as revealed by Lendrum's staining as well as qRT-PCR
83 analysis of E18.5 tissues (Fig 1A and B, Fig S1), confirming previous studies on other Lgr5-deficient
84 mouse strains [21,25]. In addition, quantification of the stem cell pool with the Olfm4 marker indicated
85 expansion of this population in the intervillus (IV) region of Lgr5 KOs as compared to that of wild-types
86 (WTs) (Fig 1C). Accordingly, Lgr5 KOs showed 4-fold increased expression of Wnt/β-catenin target
87 genes (*Ascl2*, *Axin2*), histologically detected in the IV region (Fig 1D and E). Of relevance, upregulation
88 of the truncated *Lgr5* transcript itself was even higher [10-fold versus (vs) WTs], suggesting a negative
89 control of the Lgr5 receptor on its own expression (Fig 1D). Altogether, these data suggested that Lgr5
90 deficiency generates overactivation of the Wnt/β-catenin pathway in the prenatal small intestine that
91 induces an expansion of ISC precursors and leads to premature Paneth cell differentiation around birth.

92 In attempts to reduce *in vivo* the excessive Wnt signaling tone observed in Lgr5 KO embryos, we treated
93 pregnant females (Lgr5-DTReGFP and Lgr5-GFP-Cre^{ERT2} strains) with the orally administrable Wnt
94 inhibitor LGK974. This inhibitor of the acyl transferase Porcupine (which alters Wnt ligand secretion)
95 restores normal Wnt levels in tumor-bearing mice without affecting highly proliferative tissues such as
96 the intestine [26]. Pilot experiments demonstrated that the compound efficiently crosses the placenta but
97 that its administration before embryonic stage E11.5 can affect normal embryonic development (Fig
98 S2A). Then, we tested two different administration windows for daily oral gavage (dose of 3 mg/kg/day),
99 i.e. starting before (E13-E15) or during (E15-E17) the onset of Wnt-mediated cytodifferentiation (Fig
100 2A). When analyzed at E18.5, LGK974-treated tissues did not show any major alteration in the

101 epithelium (Fig 2B). Administration of LGK974 between E15-E17, but not earlier, reduced Paneth cell
102 differentiation in Lgr5 KOs to control levels (Fig 2C, ,Fig S2B). The treatment reduced expression of
103 Wnt target genes (*Axin2*, *Ascl2*, *Lgr5 ex1*) expressed by ISCs without significantly altering expression
104 of other reported stem cell markers (*Hopx*, *Tert*) (Fig 2D, Fig. S2C). LGK974 administration also
105 induced downregulation of the Paneth cell marker *Crypt5* but not that of other cell lineages markers (Fig
106 2D, Fig. S2C). In contrast, attempts to upregulate Wnt/β-catenin signaling in *Lgr5*-expressing stem cells
107 between E15-E17 by a genetic approach *via* deletion of the β-catenin exon 3 (encoding the sequences
108 targeting the protein for proteasome degradation [27]) worsened the Paneth cell differentiation
109 phenotype in Lgr5 KO embryos as compared to Lgr5 HEs (2.29 ± 0.33 vs 1.15 ± 0.22 paneth cells/10
110 intervilli, respectively; $p=0.0317$) (Fig S2D). Together, these rescue experiments further strengthened
111 the notion that the Lgr5 receptor is involved in negative regulation of the Wnt/β-catenin activity at the
112 onset of cytodifferentiation in the embryonic intestine.

113 **Postnatal induction of Lgr5 ablation in ISCs alters stem cell fate towards the Paneth cell lineage**

114 To determine whether the phenotype observed in Lgr5-deficient embryos could be reproduced
115 postnatally (PN) when the Paneth cells normally emerge in control tissues, we generated conditional
116 deficient-Lgr5 mice (cKO). These mice are double heterozygous *Lgr5*^{GFP-CreERT2/flox} in which cre-
117 mediated deletion of Lgr5 exon 16 causes a frameshift and a null phenotype [1,17]. Following 3
118 consecutive tamoxifen injections to lactating females (PN days 6-8), we compared the fate of cKO Tom-
119 recombined cells to that of control heterozygous (HE) *Lgr5*^{GFP-CreERT2/+}/*Rosa26R*-Tom littermates after
120 10 days of chase (Fig 3A). No significant differences in terms of clone number were observed in Lgr5-
121 ablated Tom⁺ tissues as compared to controls, suggesting that stemness was preserved during this
122 period of chase (Fig 3B, C). However, cKO PN18 Lgr5-ablated Tom⁺ tissues exhibited a clear bias
123 towards Paneth cell differentiation (Fig 3B and D). Such phenotype was observed in proximal and distal
124 small intestines (Fig S3). When Lgr5 ablation was induced in adults already bearing a definitive number
125 of Paneth cells in crypts, such phenotype was not observed 1 month after recombination; and no
126 significant differences were detected in the proportion of traced clones (Fig 3B, D and E). Together,
127 these data are consistent with the fact that loss of Lgr5 function in homeostatic adult tissues is not

128 associated with an overt phenotype [17] meanwhile absence of the Lgr5 receptor during the prenatal and
129 early postnatal stages impacts on stem cell fate.

130 **Lgr5 controls extracellular matrix autocrine production in stem cells**

131 To investigate the molecular pathways altered by Lgr5 deficiency, we analyzed the transcriptomic
132 profile of GFP^{+ve} ISC precursors from Lgr5-DTReGFP HEs and KOs at E16.5. At this developmental
133 stage, potential impact of Paneth cells was excluded based on Lendum' stainings. Two pools of Lgr5
134 HEs (n= 7 and 8) and Lgr5 KOs (n= 2 and 6) coming from 2 different litters were isolated by
135 Fluorescence-Activated cell sorting (FACS). RNAseq on these samples followed by differential gene
136 expression analysis identified 487 genes (96 upregulated/391 downregulated) modulated in Lgr5 KOs
137 vs HEs (False Discovery rate 0.1 and fold change above 1.5) (Fig 4A and B). Lgr5 deficiency was
138 strikingly associated with de-enrichment in the Epithelial Mesenchymal Transition Gene dataset (47
139 genes modulated out of 200 genes in the EMT dataset, p value 4.e⁻⁶⁰) (Fig 4B and C). Gene Ontology-
140 Panther analysis of this short gene list indicated profound reorganization of the matrisome with
141 significant reduction in Extracellular matrix (ECM) structural constituents, including collagen fibrils, in
142 Lgr5-deficient ISC precursors (Fig 4B). In accordance with ECM playing a role in development [28],
143 downregulated genes were also associated with tissue development, morphogenesis and regulation of
144 cell migration (Fig 4B). Reduced expression of the Cadherin member Cdh11 and increased expression
145 of the apical junction component Claudin 4 (Cldn4) suggested enforcement of an epithelial phenotype
146 in Lgr5 KO precursors, coherent with evolution of these precursor ISCs towards a more mature stage
147 (Fig 4A). To test this hypothesis, we compared the transcriptomes of E18.5 embryos and adult Lgr5 HE
148 ISCs. Stem cell maturation was associated with downregulation of EMT processes with decreased
149 expression of ECM-associated genes (Fig 4B, 4C and S4A). Moreover, in agreement with the study of
150 Navis et al [29] investigating transcriptomic changes during suckling-to-weaning transition, maturation
151 of ISCs also involved metabolic changes: with downregulation of the neonatal-related genes *Lactase*
152 (*Lct*), *Arginosuccinate synthetase 1* (*Ass1*) and upregulation of the adult-related *Arginase 2* (*Arg2*) and
153 *Sucrase-isomaltase* genes (*Si*) (Fig S4A). Together, these findings revealed that the transcriptome of
154 ISCs substantially evolves during development, changing from an immature mesenchymal-like to a

155 definitive mature epithelial phenotype. In addition, embryos deficient for Lgr5 demonstrate an
156 accelerated conversion to an adult-type stage.

157 Transition from a mesenchymal to an epithelial phenotype is controlled by various signaling pathways
158 [30]. Consistent with an involvement of the Wnt/β-catenin pathway, Lgr5 E16.5 KO GFP^{+ve} ISCs
159 exhibited upregulation of the *Axin2*, *Bax* and *Edn1* target genes and the ISC number at E16.5 appeared
160 significantly expanded in KOs as compared to HEs (Fig 4A and D, upper right panel). Relative levels
161 of the most expressed Wnt Frizzled (Fzd5 and Fzd7) and Lrp coreceptors (Lrp6) were not significantly
162 changed by the developmental stage of ISCs or the Lgr5 expression level (HE or KO) but expression of
163 Wnt ligands varied over time (Fig 4D lower panels, Fig S4B). Indeed, expression of the non-canonical
164 Wnt5a ligand, predominant in HE ISCs at E16.5 (in agreement with data from [13]); progressively
165 dropped at a later prenatal stage (E18.5) and adulthood meanwhile expression of the canonical Wnt3
166 ligand increased in ISCs during the same period (Fig 4D, Fig S4A). In Lgr5-deficient ISCs, the Wnt5a-
167 to-Wnt3 shift expression was detected at an earlier stage (E16.5) as compared to Lgr5 HEs pairs (Fig
168 4D, lower right panel). In addition, the TGFβ pathway involved in EMT was found deregulated in
169 absence of the Lgr5 receptor with downregulation of *Bmp3* and *TGFβi* in E16.5 KOs as compared to
170 HEs (Fig 4A). Moreover, whereas the inflammatory response (involving TNFα/NFkB and IFN α/γ
171 pathways) was found upregulated during normal ISC maturation, this did not occur in E16.5 ISC KOs;
172 these cascades appearing downregulated as compared to E16.5 ISC HEs (with downregulation of *Cxcl1*,
173 *Tnfaip3*, *Cxcl10* and *Nfkbia* genes) (Fig. 4A and B). Surprisingly, when Lgr5 function was specifically
174 disrupted in adults using Lgr5^{Cre/lox} mice, most of the pathways downregulated in E16.5 KOs were
175 instead upregulated (Fig 4E). As an exception, the IFN α/γ pathway appeared similarly downregulated
176 in Lgr5-deficient embryo or adult stem cells (Fig 4E). Altogether, these data indicated that the
177 transcriptome of ISC significantly changes from prenatal to adult stage, acquiring a definitive epithelial
178 phenotype associated with: i) a net decrease in the capacity to generate its own extracellular matrix
179 niche, ii) a conversion in Wnt ligand autocrine production and iii) an increased ability to respond to
180 inflammatory signals. Moreover, absence of Lgr5 expression in the early ISC precursors (i.e. just after
181 their emergence in intervillus regions) leads to accelerated conversion of ISCs towards their epithelial

182 mature phenotype whereas acute ablation of Lgr5 in adults rather shifts epithelial stem cells towards a
183 mesenchymal-like phenotype.

184 **Stemness is preserved in Lgr5-deficient organoids *ex vivo***

185 ISC co-express the two parologue receptors Lgr4 and Lgr5 [17,31]. Since deficiency for the Lgr4
186 receptor leads to ISC loss due to insufficient Wnt signaling in cultured crypts, we assessed the long-
187 term growth properties of Lgr5-deficient ISCs in the *ex vivo* culture system [31]. Irrespective of the
188 mouse strain of origin, Lgr5 KO E18.5 small intestines generated a 3-4-fold increase in the absolute
189 number of growing organoids which exhibited higher complexity (measured by the branching
190 coefficient) as compared to WTs and HEs upon initial seeding (Fig 5A). Then, we assessed whether the
191 Wnt tone in Lgr5 KO organoids would be sufficient to confer reduced growth requirements for the
192 Rspordin 1 (Rspo1) ligand. Despite an overall 2-fold increase in Wnt signaling activity (*Axin2*, *Ascl2*,
193 *Olfm4*, *Lgr5*) at any Rspo1 concentration tested as compared to Lgr5-DTReGFP WTs, KO organoids
194 remained dependent on Rspo1 to grow *ex vivo* (Fig 5B and C). As observed in tissues, differentiation
195 towards the Paneth cell lineage was increased in Lgr5 KO cultures (Fig S5A). Since transcriptomic
196 analysis of Lgr5 KOs had suggested modifications in the stemness status of precursor ISCs, we studied
197 whether this might affect long-term maintenance of ISCs *ex vivo* by passaging Lgr5-DTReGFP samples
198 for more than 20 passages (Fig S5B). Expression of Wnt target genes was maintained over passages as
199 compared to Lgr5 WTs (Fig S5C). Together, these results indicated that long-term replating of Lgr5 KO
200 organoids is preserved *ex vivo*, without evidence of Lgr5 deficiency leading to loss of stemness.

201 **Rspordin 2 ligand/ Lgr5 receptor interaction regulates stem cell fate in organoids *ex vivo***

202 Rspordin (Rspo1/Rspo2/Rspo3/Rspo4) have been reported to behave as redundant ligands for Lgr
203 receptors, leading to enhanced Wnt/β-catenin activity [16-20]. We investigated the impact of Rspordin
204 members on organoid growth *ex vivo* by culturing Lgr5-DTReGFP WTs isolated from E18.5 small
205 intestines in the Sato medium containing EGF, Noggin plus either mRspo1 or mRspo2. Both conditions
206 allowed efficient growth of Lgr5 WT organoids after 5 days of culture (Fig 6A). However, when cultured
207 in Rspo2 medium, organoids emitted elongated protrusions as compared to those grown in the Rspo1

208 medium (Fig 6A). As assessed by qRT-PCR analysis, culture of WT organoids in mRspo2 conditions
209 induced downregulation of the stem cell markers *Ascl2* (by 70%), *Axin2* and *Olfm4* (by 30%) as well as
210 the *Lgr5* gene itself (by 40%) as compared to mRspo1 conditions (Fig 6B). Accordingly, *in situ*
211 hybridization and immunohistochemistry experiments confirmed decreased *Axin2* expression in crypt-
212 like domains and reduction in the proportion of Olfm4-expressing cells in WT organoids in Rspo2 vs
213 Rspo1 conditions (Fig 6C). In contrast to WT organoids, KO organoids did not demonstrate such
214 morphological differences in Rspo1 and Rspo2-containing media (Fig 6A). Wnt target gene expression
215 remained at higher levels in Lgr5 KO organoids as compared to WTs irrespective of the Rspordin type
216 used for culture (Fig 6B and C). Therefore, these data indicated that Rspo ligands do not exhibit
217 redundant functions on ISCs grown *ex vivo*, this likely involving the Rspo2/Lgr5 axis. Further, to
218 determine whether this interaction in ISCs can also affect cell differentiation, we analyzed the expression
219 of specific cell-lineage markers by qRT-PCR (Fig 6D). Replacement of Rspo1 by Rspo2 did not impact
220 on ChgA^{+ve} enteroendocrine or Muc2^{+ve} Goblet cell differentiation, but induced a bias towards the SI^{+ve}
221 absorptive lineage to the expense of the Crypt5^{+ve} Paneth cell type in WT organoids (Fig 6D). Analysis
222 of Lgr5-deficient organoids suggested that the Rspo2/Lgr5 interaction might control commitment
223 towards the absorptive fate but also that Rspo2 can regulate Paneth cell differentiation *via* its interaction
224 with cell surface molecules other than the sole Lgr5 receptor.

225 **DISCUSSION**

226 Since the identification of the atypical GPCR receptor Lgr5 as a bone-fide stem cell marker in the normal
227 intestinal epithelium as well as in cancer cells, the potential biological function of this receptor has been
228 questioned but still, it remains elusive and controversial [32]. The biological function of Lgr5 was
229 initially addressed in Lgr5-null embryos using the Lgr5-LacZNeo mouse line, in which exon 18 coding
230 for the transmembrane and intracellular tail, is replaced by the reporter cassette [33]. The observed
231 phenotype suggested that Lgr5 exerts a negative regulatory role on the Wnt/β-catenin pathway in stem
232 cells [32]. Following the publication of reports identifying Rspindins as ligands for Lgr5, and showing
233 that this interaction enhances Wnt/β-catenin signaling *in vitro*, we have readdressed the biological
234 relevance of this marker on two other plain knock in/knockout Lgr5eGFP-Ires-CreERT2 and Lgr5-DTR
235 mouse strains, which differ from the Lgr5-LacZNeo one by the fact that reporter cassettes are inserted
236 within the first exon of Lgr5 [1,17]. Irrespective of the mouse strain considered, the observation that
237 Wnt ligand inhibition at the onset of cytodifferentiation could interfere with the precocious Paneth cell
238 differentiation observed at birth in knockouts, further strengthened conclusions drawn from the first
239 report on a role of Lgr5 in negative regulation of the Wnt/β-catenin activity during the prenatal stage.
240 Similarly, conditional ablation of the Lgr5 function in the postnatal phase during which Paneth cell
241 differentiation normally proceeds, accelerated the maturation process. In adults, no overt phenotype was
242 observed upon Lgr5 loss (though significant transcriptomic changes were detected), likely blurred in a
243 context where Paneth cells are fully established. In addition, phenotypic differences observed in fetal
244 and adult tissues upon Lgr5 loss may also be explained by co-expression of the parologue Lgr4 receptor
245 demonstrated to play a dominant role in ISCs on Wnt signaling over Lgr5 [17,25,31]. Considering that
246 Lgr5, but not Lgr4, is a direct Wnt/β-catenin target gene, one hypothesis is that both receptors might
247 play complementary roles in ISCs, Lgr4 and Lgr5 regulating Wnt signaling under normal homeostatic
248 and Wnt overactivated situations, respectively.

249 To investigate the molecular mechanisms associated with premature Paneth cell differentiation
250 in Lgr5-deficient embryos at birth, the transcriptomes of heterozygous (control) and homozygous (KO)
251 ISCs were compared at E16.5. Deficiency for Lgr5 induced a profound downregulation of many

252 extracellular matrix (ECM) components i.e. collagens, proteoglycans (versican, decorin,), glycoproteins
253 (laminin a4, fibronectin, thrombospondins, nidogens) and ECM- associated modifying proteins (Adamts
254 proteases, Lysyl oxidase, cytokines, glycosaminoglycan-modifying heparan sulfate sulfotransferase), all
255 involved in matrisome formation and maintenance. The highly dynamic matrisome, defined by a core
256 of ~ 300 proteins localizing at the basement membrane (between epithelial cells and stromal cells) and
257 in the neighboring interstitial space, is known to regulate tissue development, as well as fibrosis and
258 cancer progression in adults [28]. Our findings provide evidences that early ISC precursors (E16.5) are
259 themselves able to synthesize their own ECM components, in particular collagen fibrils known to control
260 matrix stiffness, this conferring to these epithelial cells some kind of mesenchymal-like properties.
261 Coherent with a recent report demonstrating that softening of the matrigel in the *ex vivo* culture system
262 enhances stem cell differentiation in adult ISC-derived organoids, we observed that decreased
263 expression of ECM proteins by E16.5 KO ISCs, likely reducing stiffness of the tissue surrounding ISCs,
264 correlated with precocious differentiation of Paneth cells before birth [34]. Moreover, according to our
265 transcriptomic data on adult vs embryonic ISCs, the capacity of stem cells to synthesize their own ECM
266 components progressively decreases during maturation, correlating with acquisition of a definitive
267 “fully” epithelialized phenotype. In the adult intestinal crypt, the ISC microenvironment substantially
268 differs from the prenatal intervillus domains, in particular through its cellular niche composed of
269 adjacent epithelial Paneth cells as well as various resident stromal cell types, which all might contribute
270 to provide the adequate ECM environment to ISCs [14,35-36]. Nevertheless, based on our transcriptome
271 analyses of ISCs depleted of Lgr5 ($Lgr5^{Cre/flx}$ vs $Lgr5^{Cre/+}$), adult ISCs still conserve the control on their
272 epithelial status as loss of the Lgr5 receptor favored transition from an epithelial to a more mesenchymal-
273 like phenotype (EMT Hallmark upregulated in KOs vs HEs). In line with these findings obtained under
274 *in vivo* homeostasis, Lgr5 knockdown on cultured colorectal cancer cell lines also leads to upregulation
275 of EMT-related genes *in vitro* [37]. These results, linking Lgr5 function to EMT control in adult ISCs,
276 highlight the interest to conduct further studies addressing the role of this receptor on the metastatic
277 potential of cancer cells. Our study also sheds new lights regarding molecular mechanisms associated
278 with ISC maturation. Indeed, in addition to Wnt signaling, other pathways were identified to be
279 modulated in ISCs during this process, in particular the inflammatory response that was induced in

280 adults vs E18.5 ISCs. Remarkably, in E16.5 Lgr5-null ISCs, transcriptome data suggested that the
281 TNF α , and IFN α/γ pathways, well known to crosstalk with the Wnt cascade in a complex way, appeared
282 downregulated as compared to control ISCs [38-39]. Future studies will be needed to determine if ISC
283 maturation in Lgr5-null embryos, is not only accelerated but also improperly executed in this regard.

284 Initial *in vitro* studies, identifying Rspindins (Rspo1/Rspo2/Rspo3/Rspo4) as ligands for the
285 three Lgr paralogues, suggested both ligand and receptor redundancy [16-19]. However, evidences have
286 been provided that Rspo2, but not other members of this family, exhibits tumor suppressive activity on
287 colorectal cancer cell lines *via* negative regulation of the Wnt/ β -catenin pathway through interaction
288 with the Lgr5 receptor [20]. In order to clarify this point, we compared the effect of Rspo1 and Rspo2
289 on ISC growth and differentiation in the *ex vivo* culture system. As compared to Rspo1, Rspo2
290 downregulated expression of ISC gene markers (*Ascl2*, *Olfm4*, *Lgr5*, *Sox9*, *Axin2*) in WT organoids, and
291 differentially modulated cell lineage commitment (essentially affecting the Absorptive and Paneth
292 lineages). The observation that ISC markers remained at similar higher levels in Lgr5-deficient
293 organoids irrespective of the Rspindin used as compared to WTs, this is consistent with Rspo2
294 ligand/Lgr5 receptor interaction specifically negatively controlling the Wnt/ β -catenin pathway in ISCs.
295 Nevertheless, the observed effect of Rspo2 vs Rspo1 towards the Paneth cell lineage on Lgr5-null
296 organoids might also be explained by interaction of Rspo2 with other receptors, possibly the cognate
297 Lgr4 receptor or likely heparan sulfate proteoglycans, such as Glypican or Syndecan receptors (namely
298 Gpc3/Gpc4 and Sdc1/Sdc4 that are the most expressed in ISCs-Fig S4B). These latter cell surface
299 molecules have recently been reported as alternative receptors for Rspo2 and Rspo3 to regulate Wnt/ β -
300 catenin signaling [40-41]. *In vivo*, the main source of these ligands are peri-cryptal myofibroblasts,
301 which predominantly express Rspo3 under normal conditions and can overexpress Rspo2 upon infection
302 or inflammatory stimuli [42-43]. Considering this complex ligand expression pattern and that of the
303 known receptors, it is tempting to speculate that regulation of the ISC fate through Rspo/Lgrs interaction
304 might depend in part on both spatial and temporal release of Rspo ligands in the ISC niche.

305 **MATERIAL AND METHODS**

306 *Experimental animals*

307 Animal procedures complied with the guidelines of the European Union and were approved by the local
308 ethics committee under the accepted protocols 535N and 631N. Mice strains were: *Lgr5*-DTR knock-in
309 [24], *Ctnnb1*^{exon3} [27], *Lgr5*-LacZNeo [33], *Lgr5*-Flox exon16 [17], *Lgr5*-GFP-Cre^{ERT2} [1]. Rosa26CAG
310 floxed stop *tdTomato* referred as Rosa26R-Tomato and *Axin2*-LacZ (Jax mice). The day the vaginal
311 plug was observed was considered as embryonic day 0.5 (E0.5).

312 For LGK974 rescue experiments, pregnant females were administered the LGK974 compound (kindly
313 provided by Novartis) by oral gavage once a day at a dose of 1-3 mg/kg/day.

314 For lineage tracing experiments, tamoxifen (Sigma-Aldrich) was dissolved in a sunflower oil (Sigma-
315 Aldrich)/ethanol mixture (9:1) at 10 mg/ml and used at a dose of 0.1 mg/g of body weight for gestating
316 and lactating females or at a single dose of 2 mg for adult mice by intra-peritoneal injection.

317 *Tissue processing and immunohistochemical analysis*

318 Small intestine samples were immediately fixed with 10% formalin solution, neutral buffered (Sigma-
319 Aldrich) overnight at +4°C and then sedimented through 30% sucrose solution before OCT embedding.

320 Histological and X-gal staining protocols as well as immuno-fluorescence/histochemistry experiments
321 on 6 µm sections were carried out as previously described [21]. Lendrum's staining was performed
322 according to the manufacturer's instructions (cat # 631340, Clinitech, UK). The primary antibodies used
323 for staining were: rabbit anti-Olfm4 (Cell Signaling), rabbit anti-Plyz (Dako), rat anti-RFP (Chromotek),
324 mouse anti-beta-catenin BD). Samples were visualized with Zeiss Axioplan 2 (immunohistochemistry)
325 or Zeiss Observer Z1 microscope (immunofluorescence).

326 Quantification of the number of Paneth cells per 10 intervillus units (IV) was performed on a mean of
327 50 IV in E18.5 tissues, on a mean of 20 and 100 Tomato-recombined crypts in postnatal and adult
328 samples. Postnatal and adult lineage tracing analysis was performed on a mean of 100 crypt-villus units.
329 Quantification of Olfm4^{+ve} cells per IV was performed on a minimum of 20 IV per embryo. The number
330 of animals used for each experiment is reported in Figure legends.

331

332

333 *Ex vivo culture*

334 Embryonic small intestine was dissociated with 5 mM EDTA-in DPBS (Gibco) according to the
335 protocol reported in [44]. Briefly, the culture medium used consisted in Advanced-DMEM/F12 medium
336 supplemented with 2 mM L-Glutamine, N2 and B27 w/o vit.A (Invitrogen), gentamycin, penicillin-
337 streptomycin cocktail, 10 mM HEPES, and 1 mM N acetyl cysteine. Growth factors were added at a
338 final concentration of : 50 ng/ml EGF and 100 ng/ml Noggin (both from Peprotech), and 100 ng/ml
339 CHO-derived mouse R-spondin 1 or 5 ng/ml CHO-derived mouse R-spondin 2 (R&D System). The
340 final concentration of R-spondins in the culture medium was initially tested in pilot experiments in order
341 to add comparable amounts of bioactive ligands (bioactivity measured by TOPflash assays and organoid
342 growth curves, R&D systems). Culture medium was changed each other day and after 5-6 days in
343 culture, organoids were harvested, mechanically dissociated and replated in fresh Matrigel (BD
344 Biosciences). Culture media were supplemented with 10- μ M Y-27632 (Sigma Aldrich) in all initial
345 seeding and replating experiments. Pictures were acquired with a Moticam Pro camera connected to
346 Motic AE31 microscope.

347 *Gene expression analysis*

348 qRT-PCR was performed on total RNA extracted from embryonic tissues or organoid cultures as
349 reported [21]. Expression levels were normalized to that of reference genes (Rpl13, Gapdh, Ywhaz).
350 Each sample was run in duplicate. Primer sequences are reported in Table S1. *In situ* hybridization
351 experiments were performed using the MmAxin2 RNAscope probe (cat # 400331, ACD, UK) according
352 to manufacturer instructions with the RNAscope kit.

353 *RNA seq and Gene Set Enrichment Analysis (GSEA)*

354 RNA quality was checked using a Bioanalyzer 2100 (Agilent technologies). Indexed cDNA libraries
355 were obtained using the Ovation Solo RNA-Seq System (NuGen) following manufacturer
356 recommendation. The multiplexed libraries were loaded on a NovaSeq 6000 (Illumina) using a S2 flow
357 cell and sequences were produced using a 200 Cycle Kit. Paired-end reads were mapped against the
358 mouse reference genome GRCm38 using STAR software to generate read alignments for each sample.
359 Annotations Mus_musculus.GRCm38.90.gtf were obtained from ftp.ensembl.org. After transcripts
360 assembling, gene level counts were obtained using HTSeq. Genes differentially expressed were

361 identified with EdgeR method (FDR 0.1 and Fold change 1.5) and hallmarks were analyzed using GSEA
362 MolSig (Broad Institute) [45]. Then, Gene pattern was used to compare by pre-ranked GSEA E16.5
363 Lgr5 KO vs HE; Adult HE vs E18.5 HE, or Adult Lgr5 KO vs HE transcriptomes with Gene data sets
364 [46]. Gene Ontology was used to identify biological processes [47]. Transcript profiling: GEO accession
365 number will be communicated upon publication.

366 *Statistical analysis*

367 Statistical analyses were performed with Graph Pad Prism 5. All experimental data are expressed as
368 mean \pm s.e.m. The significance of differences between groups was determined by appropriate parametric
369 or non-parametric tests as described in Figure legends.

370 **Acknowledgments**

371 We are grateful to Genentech for providing us with the *Lgr5*-DTReGFP mice, Novartis for providing
372 LGK974 compound, Makoto Taketo for providing the *Ctnnb1* exon3 strain and Hans Clevers for
373 providing the *Lgr5*-LacZNeo and *Lgr5* flox mouse strains.

374 Grant support: supported by the Interuniversity Attraction Poles Programme-Belgian State-Belgian
375 Science Policy (6/14), the Fonds de la Recherche Scientifique Médicale of Belgium, the Walloon Region
376 (program CIBLES) and the non-for-profit Association Recherche Biomédicale et Diagnostic.

377 **Author contributions:**

378 VFV, study concept and design, acquisition of data, analysis and interpretation of data, statistical
379 analysis, drafting of the ms

380 ML, RG, DRS, AL, FL: acquisition of data, analysis and interpretation of data, statistical analysis
381 GV: study concept and design, critical revision of the ms, obtained funding, study supervision
382 MIG: study concept and design, acquisition of data, analysis and interpretation of data, drafting of the
383 ms, critical revision of the ms, study supervision

384 **Conflict of interest:** The authors have nothing to disclose

385 **References**

- 386 1. Barker N, van Es JH, Kuipers J, Kujala P, van den Born M, et al. (2007) Identification of stem
387 cells in small intestine and colon by marker gene Lgr5. *Nature* 449: 1003-1007.
- 388 2. Fernandez-Vallone V, Garcia MI (2016) Stem Cells in Adult Homeostasis, Regeneration and
389 Tissue Development of the Digestive Tract Epithelium. *Int J Stem Cell Res Ther*, 3:038.
- 390 3. Takeda N1, Jain R, LeBoeuf MR, Wang Q, Lu MM, Epstein JA. (2011). Interconversion
391 between intestinal stem cell populations in distinct niches. *Science* 334: 1420-1424.
- 392 4. Yan KS, Chia LA, Li X, Ootani A, Su J, Lee JY, Su N, Luo Y, Heilshorn SC, Amieva MR,
393 Sangiorgi E, Capecchi MR, Kuo CJ. (2012). The intestinal stem cell markers Bmi1 and Lgr5
394 identify two functionally distinct populations. *Proc Natl Acad Sci U S A* 109: 466-471.
- 395 5. Metcalfe C, Kljavin NM, Ybarra R, de Sauvage FJ. (2014) Lgr5+ stem cells are indispensable
396 for radiation-induced intestinal regeneration. *Cell Stem Cell* 14: 149-59.
- 397 6. Gao N, White P, Kaestner KH (2009) Establishment of intestinal identity and epithelial-
398 mesenchymal signaling by Cdx2. *Dev Cell*. 16: 588-99.
- 399 7. Kumar N, Tsai YH, Chen L, Zhou A, Banerjee KK, Saxena M, Huang S, Toke NH, Xing J,
400 Shivedasani RA, Spence JR, Verzi MP (2019) The lineage-specific transcription factor CDX2
401 navigates dynamic chromatin to control distinct stages of intestine development. *Development*.
402 146: dev172189.
- 403 8. Walton KD, Freddo AM, Wang S, Gumucio DL (2016) Generation of intestinal surface: an
404 absorbing tale. *Development*. 143: 2261-72.
- 405 9. Dehmer JJ, Garrison AP, Speck KE, Dekaney CM, Van Landeghem L, Sun X, Henning SJ,
406 Helmrath MA (2011) Expansion of intestinal epithelial stem cells during murine development.
407 *PLoS One*. 6: e27070.
- 408 10. Korinek V, Barker N, Moerer P, van Donselaar E, Huls G, Peters PJ, Clevers H (1998) Depletion
409 of epithelial stem-cell compartments in the small intestine of mice lacking Tcf-4. *Nat
410 Genet*. 1998 Aug;19(4):379-83.
- 411 11. Mustata RC, Vasile G, Fernandez-Vallone V, Strollo S, Lefort A, Libert F, Monteyne D, Pérez-
412 Morgia D, Vassart G, Garcia MI (2013) Identification of Lgr5-independent spheroid-generating
413 progenitors of the mouse fetal intestinal epithelium. *Cell Rep* 5: 421-32.
- 414 12. Kim TH, Escudero S, Shivedasani RA (2012) Intact function of Lgr5 receptor-expressing
415 intestinal stem cells in the absence of Paneth cells. *Proc Natl Acad Sci U S A* 109: 3932-7.
- 416 13. Nigmatullina L, Norkin M, Dzama MM, Messner B, Sayols S, Soshnikova N (2017) Id2
417 controls specification of Lgr5+ intestinal stem cell progenitors during gut development. *EMBO
418 J* 36: 869-885.

419 14. Sato T, Vries RG, Snippert HJ, van de Wetering M, Barker N, Stange DE, van Es JH, Abo A,
420 Kujala P, Peters PJ, Clevers H (2009) Single Lgr5 stem cells build crypt-villus structures in
421 vitro without a mesenchymal niche. *Nature* 459: 262-5.

422 15. Hans Clevers (2013) The Intestinal Crypt, A Prototype Stem Cell Compartment. *Cell* 154: 274-
423 84.

424 16. Carmon KS, Gong X, Lin Q, Thomas A, Liu Q (2011) R-spondins function as ligands of the
425 orphan receptors LGR4 and LGR5 to regulate Wnt/beta-catenin signaling. *Proc Natl Acad Sci
426 U S A* 108: 11452-7.

427 17. de Lau W, Barker N, Low TY, Koo BK, Li VS, Teunissen H, Kujala P, Haegebarth A, et al
428 (2011) Lgr5 homologues associate with Wnt receptors and mediate R-spondin signalling.
429 *Nature* 476: 293-7.

430 18. Glinka A, Dolde C, Kirsch N, Huang YL, Kazanskaya O, Ingelfinger D, Boutros M, Cruciat
431 CM, Niehrs C (2011) LGR4 and LGR5 are R-spondin receptors mediating Wnt/β-catenin and
432 Wnt/PCP signalling. *EMBO Rep* 12: 1055-61.

433 19. Ruffner H, Sprunger J, Charlat O, Leighton-Davies J, Grosshans B, Salathe A, Zietzling S, Beck
434 V, et al (2012) R-Spondin potentiates Wnt/β-catenin signaling through orphan receptors LGR4
435 and LGR5. *PLoS One* 7: e40976.

436 20. Wu C, Qiu S, Lu L, Zou J, Li WF, Wang O, Zhao H, Wang H, Tang J, Chen L, Xu T, Sun Z,
437 Liao W, Luo G, Lu X (2014) RSPO2-LGR5 signaling has tumour-suppressive activity in
438 colorectal cancer. *Nat Commun* 5: 3149.

439 21. Garcia MI, Ghiani M, Lefort A, Libert F, Strollo S, Vassart G (2009) LGR5 deficiency
440 deregulates Wnt signaling and leads to precocious Paneth cell differentiation in the fetal
441 intestine. *Dev Biol* 331: 58-67.

442 22. Carmon KS, Gong X, Yi J, Thomas A, Liu Q (2014) RSPO-LGR4 functions via IQGAP1 to
443 potentiate Wnt signaling. *Proc Natl Acad Sci U S A* 111: E1221-9.

444 23. Snyder JC, Rochelle LK, Ray C, Pack TF, Bock CB, Lubkov V, Lyerly HK, Waggoner AS,
445 Barak LS, Caron MG (2017) Inhibiting clathrin-mediated endocytosis of the leucine-rich G
446 protein-coupled receptor-5 diminishes cell fitness. *J Biol Chem* 292: 7208-7222.

447 24. Tian H, Biehs B, Warming S, Leong KG, Rangell L, Klein OD, de Sauvage FJ (2011) A reserve
448 stem cell population in small intestine renders Lgr5-positive cells dispensable. *Nature* 478: 255-
449 9.

450 25. Kinzel B, Pikolek M, Orsini V, Sprunger J, Isken A, Zietzling S, Desplanches M, Dubost V,
451 Breustedt D, Valdez R, Liu D, Theil D, Müller M, Dietrich B, Bouwmeester T, Ruffner H,
452 Tchorz JS (2014) Functional roles of Lgr4 and Lgr5 in embryonic gut, kidney and skin
453 development in mice. *Dev Biol* 390: 181-90.

454 26. Liu J, Pan S, Hsieh MH, Ng N, Sun F, Wang T, Kasibhatla S, Schuller AG, et al (2013)
455 Targeting Wnt-driven cancer through the inhibition of Porcupine by LGK974. *Proc Natl Acad*
456 *Sci U S A* 110: 20224-9.

457 27. Harada N, Tamai Y, Ishikawa T, Sauer B, Takaku K, Oshima M, Taketo MM (1999) Intestinal
458 polyposis in mice with a dominant stable mutation of the beta-catenin gene. *EMBO J* 18: 5931-
459 42.

460 28. Bonnans C, Chou J, Werb Z (2014) Remodelling the extracellular matrix in development and
461 disease. *Nat Rev Mol Cell Biol* 15: 786-801

462 29. Navis M, Martins Garcia T, Renes IB, Vermeulen JL, Meisner S, Wildenberg ME, van den
463 Brink GR, van Elburg RM, Muncan V (2018) Mouse fetal intestinal organoids: new model to
464 study epithelial maturation from suckling to weaning. *EMBO Rep* 20. pii: e46221.

465 30. Lamouille S, Xu J, Deryck R (2014) Molecular mechanisms of epithelial-mesenchymal
466 transition. *Nat Rev Mol Cell Biol* 15: 178-96.

467 31. Mustata RC, Van Loy T, Lefort A, Libert F, Stollo S, Vassart G, Garcia MI (2011) Lgr4 is
468 required for Paneth cell differentiation and maintenance of intestinal stem cells ex vivo. *EMBO*
469 *Rep* 12: 558-64.

470 32. Garcia MI (2017) LGRs receptors as peculiar GPCRs involved in cancer. *J Stem Cell Res Med*
471 DOI: 10.15761/JSCRM.1000116.

472 33. Morita H, Mazerbourg S, Bouley DM, Luo CW, Kawamura K, Kuwabara Y, Baribault H, Tian
473 H, Hsueh AJ (2004) Neonatal lethality of LGR5 null mice is associated with ankyloglossia and
474 gastrointestinal distension. *Mol Cell Biol* 24: 9736-43.

475 34. Gjorevski N, Sachs N, Manfrin A, Giger S, Bragina ME, Ordóñez-Morán P, Clevers H, Lutolf
476 MP (2016) Designer matrices for intestinal stem cell and organoid culture. *Nature* 539: 560-
477 564.

478 35. Meran L, Baulies A, Li VSW (2017) Intestinal Stem Cell Niche: The Extracellular Matrix and
479 Cellular Components. *Stem Cells Int* 2017:7970385.

480 36. Aoki R, Shoshkes-Carmel M, Gao N, Shin S, May CL, Golson ML, Zahm AM, Ray M, Wiser
481 CL, Wright CV, Kaestner KH (2016) Foxl1-expressing mesenchymal cells constitute the
482 intestinal stem cell niche. *Cell Mol Gastroenterol Hepatol* 2: 175-188.

483 37. Walker F, Zhang HH, Odorizzi A, Burgess AW (2011) LGR5 is a negative regulator of
484 tumourigenicity, antagonizes Wnt signalling and regulates cell adhesion in colorectal cancer
485 cell lines. *PLoS One* 6: e22733.

486 38. Ma B, Hottiger MO (2016) Crosstalk between Wnt/β-Catenin and NF-κB Signaling Pathway
487 during Inflammation. *Front Immunol* 7: 378.

488 39. Bradford EM, Ryu SH, Singh AP, Lee G, Goretsky T, Sinh P, Williams DB, Cloud AL et al
489 (2017) Epithelial TNF receptor signaling promotes mucosal repair in inflammatory bowel
490 disease. *J Immunol* 199: 1886-1897.

491 40. Lebensohn AM, Rohatgi R (2018) R-spondins can potentiate WNT signaling without LGRs.
492 Elife 7. pii: e33126.

493 41. Park S, Cui J, Yu W, Wu L, Carmon KS, Liu QJ (2018) Differential activities and mechanisms
494 of the four R-spondins in potentiating Wnt/β-catenin signaling. J Biol Chem 293: 9759-9769.

495 42. Kabiri Z, Greicius G, Madan B, Biechele S, Zhong Z, Zaribafzadeh H, Edison, Aliyev J, Wu Y,
496 Bunte R, Williams BO, Rossant J, Virshup DM (2014) Stroma provides an intestinal stem cell
497 niche in the absence of epithelial Wnts. Development 141: 2206-15.

498 43. Kang E, Yousefi M, Gruenheid S (2016) R-Spondins are expressed by the intestinal stroma and
499 are differentially regulated during *Citrobacter rodentium*- and DSS-induced colitis in mice.
500 PLoS One 11: e0152859.

501 44. Vallone, V. F., Leprovots, M., Vassart, G. and Garcia, M. (2017) *Ex vivo* culture of fetal mouse
502 gastric epithelial progenitors. *Bio-protocol* 7: e2089. DOI: 10.21769/BioProtoc.2089.

503 45. Subramanian A, Tamayo P, Mootha VK, Mukherjee S, Ebert BL, Gillette MA, Paulovich A,
504 Pomeroy SL et al (2005) Gene set enrichment analysis: A knowledge-based approach for
505 interpreting genome-wide expression profiles. PNAS 102: 15545-15550.

506 46. Reich M, Liefeld T, Gould J, Lerner J, Tamayo P, Mesirov JP (2006) GenePattern 2.0 *Nature*
507 *Genetics* 38, 5: pp500-501.

508 47. Mi H, Muruganujan A, Thomas PD (2013) PANTHER in 2013: modeling the evolution of gene
509 function, and other gene attributes, in the context of phylogenetic trees. Nucleic Acids Res 41:
510 D377-86.

511 **FIGURE LEGENDS**

512 **Figure 1. Lgr5 deficiency induces early Paneth cell differentiation and stem cell expansion in**
513 **the small intestine at E18.5.**

514 A. Paneth cell quantification on Lgr5-DTReGFP duodenum (Duo) and Ileum (Ile). Left panel:
515 Representative images of Lendum's staining. Arrows show differentiated Paneth cells. Right panel:
516 quantification of the number of cells per 10 intervillus region. Each dot indicates the value for a
517 given embryo.

518 B. Expression analysis by qRT-PCR of the indicated Paneth cell markers in Lgr5-DTReGFP ileums
519 (n= 3 WT, 6 HE, 6 KO).

520 C. Immunofluorescence showing Olfm4^{+ve} cells in Lgr5-DTReGFP duodenums. Cell nuclei were
521 counterstained with DAPI. Quantification of Olfm4^{+ve} cells per intervillus (IV) region in Duo and
522 Ile. Each dot indicates the value for a given embryo.

523 D. Gene expression analysis by qRT-PCR of the indicated stem cell markers in Lgr5-DTReGFP
524 ileums (n= 3 WT, 6 HE, 6 KO).

525 E. Axin2/LacZ expression detected by X-gal staining in Axin2^{Lac/+}-Lgr5-GFP-CreERT2 WT or
526 KO ileums.

527 Data information: All scale bars, 20 μ m. Data are represented as means \pm sem. *P< 0.05; ***P<
528 0.001; ****P< 0.0001 by Kruskal-Wallis test followed by Dunns multiple comparison test (A, B,
529 D) and by Mann-Whitney test (C).

530 **Figure 2. In utero inhibition of Wnt activity counteracts early Paneth cell differentiation**
531 **induced by Lgr5 deficiency.**

532 A. Design of the experiment. Gestating females were vehicle- or LGK974-treated by oral gavage
533 between E13-E15 or E15-E17. Small intestines of treated embryos were analyzed at E18.5.

534 B. Immunofluorescence showing β -catenin expression in Lgr5-DTReGFP ileums. Cell nuclei were
535 counterstained with DAPI.

536 C. Paneth cell quantification on Lgr5-DTReGFP ileums. Each dot indicates the value for a given
537 embryo (n= 3 to 11 embryos per condition).

538 D. Gene expression analysis by qRT-PCR of the indicated stem cell and differentiation markers in
539 Lgr5-DTReGFP ileums (vehicle-treated 7 WT and 7 KO; LGK974-treated 3 WT and 7 KO).

540 Data information: All scale bars, 20 μ m. Data are represented as means \pm sem. ns not significant,
541 **P< 0.01; ***P< 0.001 by Kruskal-Wallis test followed by Dunns multiple comparison test (C, D).

542 **Figure 3. Postnatal Lgr5 ablation in ISCs alters stem cell fate towards the Paneth cell lineage.**

543 A. Schematic representation of the genetic elements for lineage tracing during postnatal
544 development and adult homeostasis.

545 B. Representative immunofluorescence pictures showing Paneth cells (Plyz^{+ve}) in traced clones
546 (RFP^{+ve}) from control (Lgr5^{Cre/+}) and cKO (Lgr5^{Cre/flox}) ileums. Cell nuclei were counterstained with
547 DAPI.

548 Left panels: Lactating females were tamoxifen (Tam)-treated between PN 6 and PN 8. Small
549 intestines of treated pups were analyzed 10 days after the last injection (PN day 18); Right panels:
550 Adult mice received one single Tam intraperitoneal injection and ileums were analyzed 30 days
551 later.

552 C. Quantification of the number of traced clones per recombined surface in PN18-old mice. Each
553 dot indicates the value for a given mouse.

554 D. Quantification of the number of Paneth cell number per recombined RFP^{+ve} crypt on Control and
555 cKO ileums in PN18 and adult mice. Each dot indicates the value for a given mouse.

556 E. Quantification of the percentage of recombined crypts in adult mice. Each dot indicates the value
557 for a given mouse.

558 Data information: All scale bars, 20 μ m. Data are represented as means \pm sem. ns, not significant,
559 **P< 0.01 versus controls by Kruskal-Wallis test followed by Dunns multiple comparison test (C).
560 by Mann-Whitney test (D) and unpaired t test (E).

561 **Figure 4. Transcriptome analysis of Lgr5-deficient ISC precursors.**

562 A. Design of the experiment. ISC (eGFP^{+ve}) cells were sorted by FACS from Lgr5-DTReGFP
563 embryos at E16.5 and RNA extracted was subject to RNAseq analysis. Heatmap of differentially
564 regulated genes in the two independent pools (1,2) of HE and KO ISCs at E16.5.

565 B. Design of the experiment. Compared Hallmark MSigDB gene set analysis on upregulated and
566 downregulated genes in eGFP⁺ve cells isolated from Lgr5 KOs vs Lgr5 HEs at E16.5 and Lgr5 adults
567 vs E18.5 HEs. Below: GeneOntology analysis of downregulated genes identified in the Epithelial
568 Mesenchymal Transition Gene Set.

569 C. GSEA showing enrichment of the EMT data set in E16.5 Lgr5 KOs vs E16.5 HEs, adult HEs vs
570 E18.5 HE embryos, and adult Lgr5 cKO vs Lgr5 HE modulated genes. NES: Normalized
571 Enrichment Score.

572 D. Upper left: in situ hybridization showing Axin2 expression in the duodenum of E16.5 Lgr5-
573 DTReGFP embryos; Upper right: quantification of the number of eGFP⁺ve (ISC) cells per small
574 intestine at the indicated developmental stages in Lgr5 HEs and Lgr5 KOs. Each dot indicates the
575 value for a given embryo. Below left: graph showing relative expression of the Wnt ligands at
576 different developmental stages E16.5, E18.5 and adult HEs; Below right: graph showing relative
577 expression of the main Wnt ligands in Lgr5 KOs and HEs at E16.5.

578 E. Compared Hallmarks for upregulated and downregulated genes in the transcriptome of E16.5
579 Lgr5 KOs vs E16.5 HEs and Adult Lgr5-Cre cKO vs HEs.

580 Data information: Scale bar, 100 μ m. Data are represented as means \pm sem. **P< 0.01; ****P<0.001
581 Two-way ANOVA followed by Tukey's multiple comparisons test (D).

582 **Figure 5. Stemness is preserved in Lgr5-deficient organoids.**

583 A. Plating efficiency and organoid complexity of ex vivo cultured E18.5 small intestines (the
584 number of embryos analyzed is indicated in the graph). Pictures were acquired 6 days after initial
585 seeding.

586 B. Influence of mouse Rspordin 1 concentration on growth of replated Lgr5-DTReGFP WT and
587 Lgr5 KO organoids after 5 days of culture.

588 C. Gene expression analysis by qRT-PCR of the indicated stem cell markers in Lgr5-DTReGFP WT
589 and Lgr5 KO organoids at the indicated Rspordin 1 concentrations after 5 days of culture. Each dot
590 indicates the value for an organoid culture originating from a given embryo.

591 Data information: Scale bar, 50 μ m. Data are represented as means \pm sem. *P<0.05; **P< 0.01;
592 ***P<0.001. Kruskal-Wallis test, followed by Dunn's multiple comparison test (A, C).

593 **Figure 6. Rspordin 2/Lgr5 interaction regulates stem cell fate in organoids.**

594 A. Influence of Rspordin type (Rspo1 or Rspo2) on growth of replated Lgr5-DTReGFP WT and
595 Lgr5 KO organoids. Insets a and b correspond to higher magnification of the representative pictures
596 showing elongated crypt-like domains in Lgr5 WT/Rspo2 cultures. Quantification of the differences
597 in morphology of organoids after 5 days of culture.

598 B. Gene expression analysis by qRT-PCR of the indicated stem cell markers in Lgr5-DTReGFP WT
599 and Lgr5 KO organoids after 5 days of culture. Each dot indicates the value for an organoid culture
600 originating from a given embryo.

601 C. Left panel: in situ hybridization showing Axin2 expression in Lgr5-DTReGFP WT and KO
602 organoids cultured in Rspo1 or Rspo2-containing medium; right panel: immunofluorescence
603 showing Olfm4⁺ cells in Lgr5-DTReGFP WT and KO organoids. Epithelium is delineated with β -
604 catenin and nuclei counterstained with DAPI (Merge). The white arrowhead evidences accumulated
605 Olfm4 in the luminal side of organoids.

606 D. Gene expression analysis by qRT-PCR of the indicated lineage specific markers in Lgr5-
607 DTREeGFP WT and KO organoids after 5 days of culture. Each dot indicates the value for an
608 organoid culture originating from a given embryo.

609 Data information: Scale bars, 100 μ m (A) and 50 μ m (C). Data are represented as means \pm sem. ns=
610 not significant; *P< 0.05; **P< 0.01; ***P< 0.001. by Kruskall-Wallis test followed by Dunns
611 multiple comparison test (A); and by Two-way ANOVA followed by Tukey's multiple comparisons
612 test (B,D).

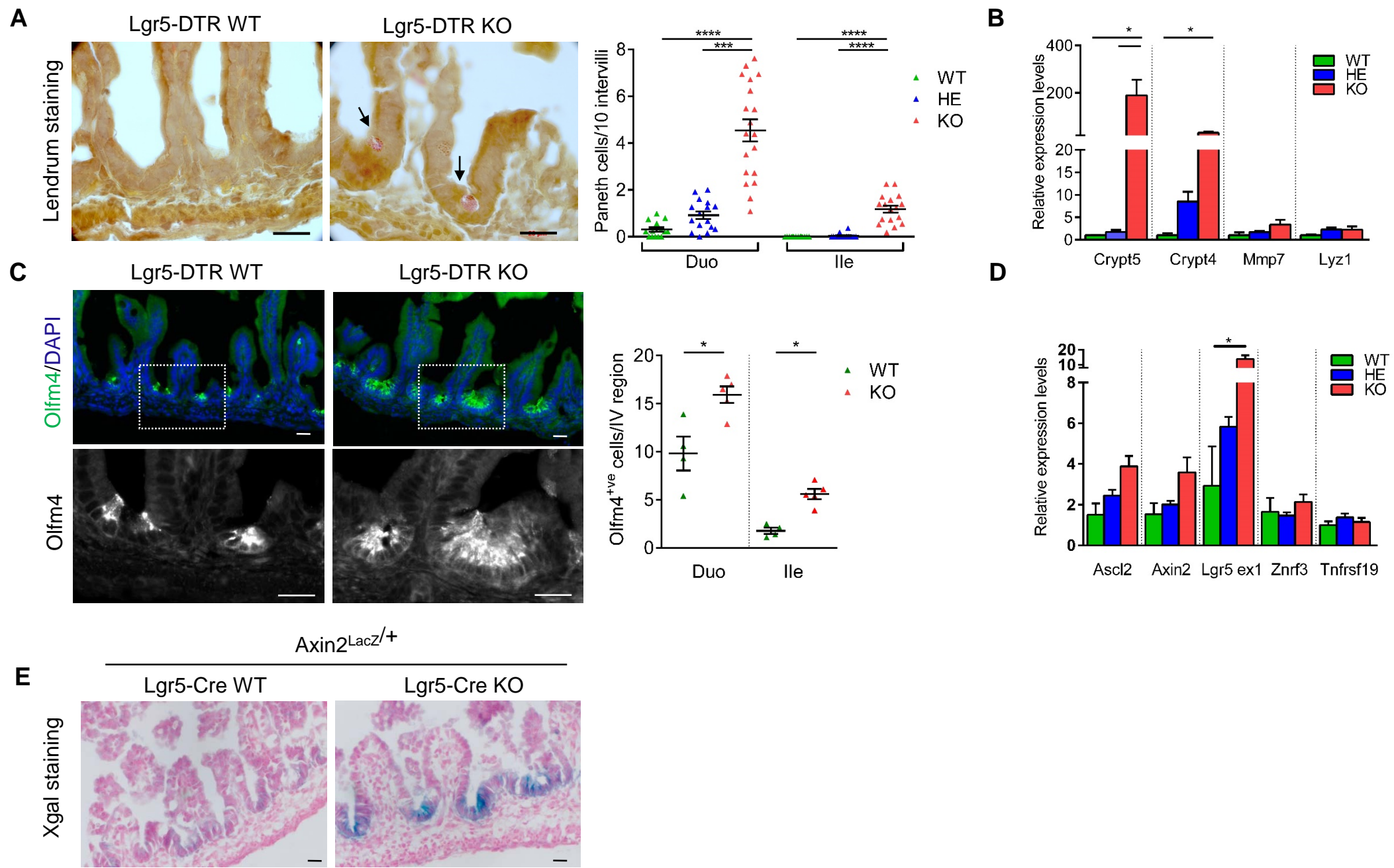
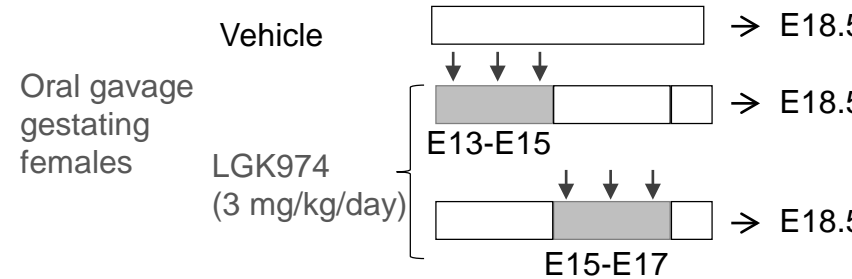
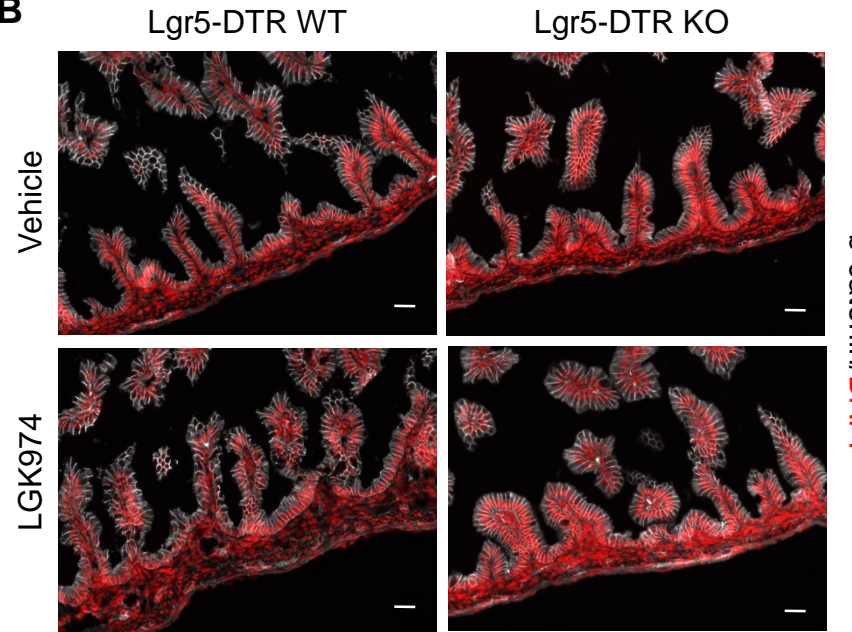
Figure 1

Figure 2

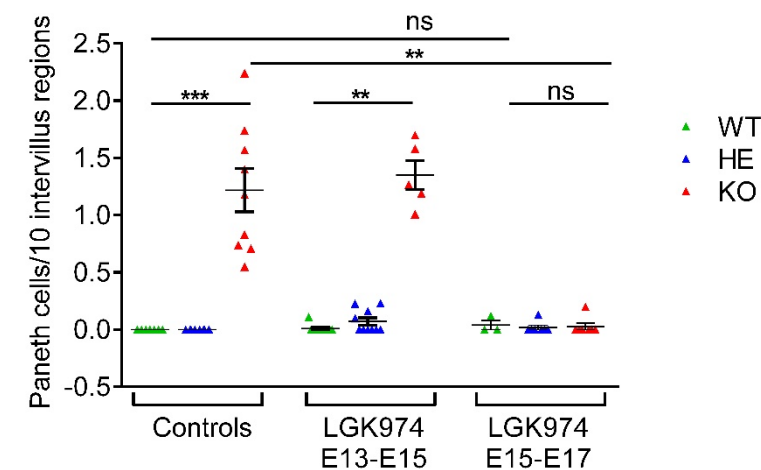
A



B



C



D

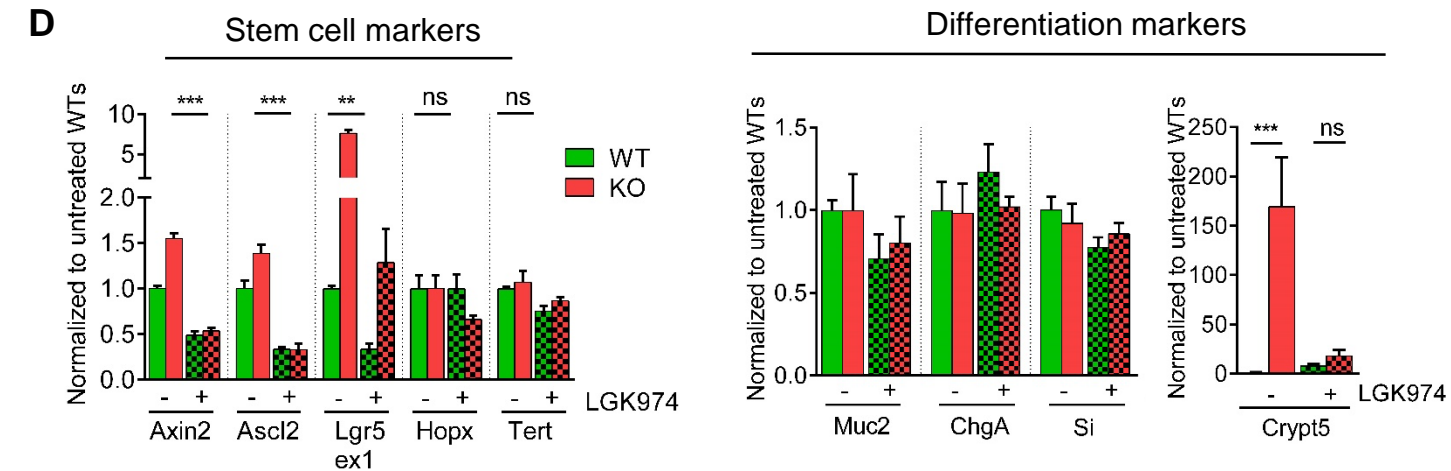
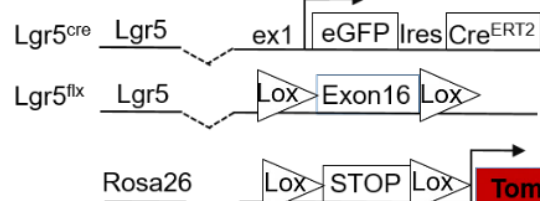
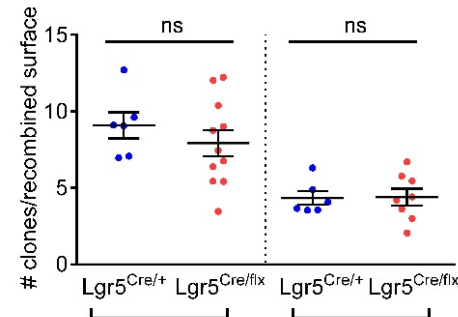


Figure 3

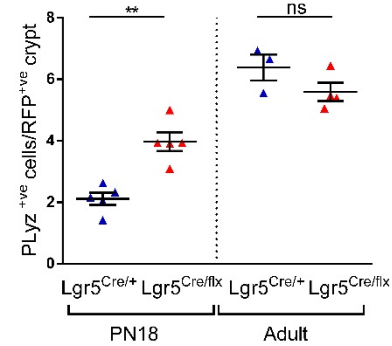
A



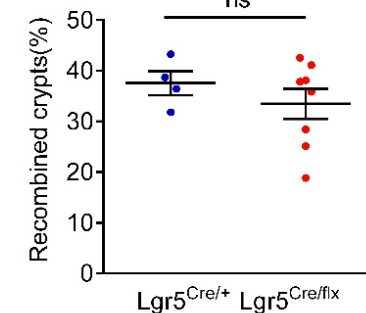
C



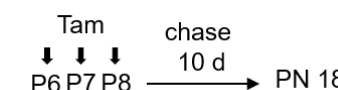
D



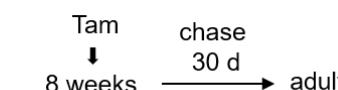
E



B

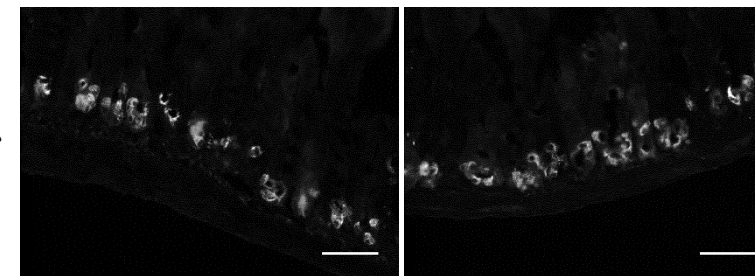


Lgr5^{Cre/+} Lgr5^{Cre/flx}

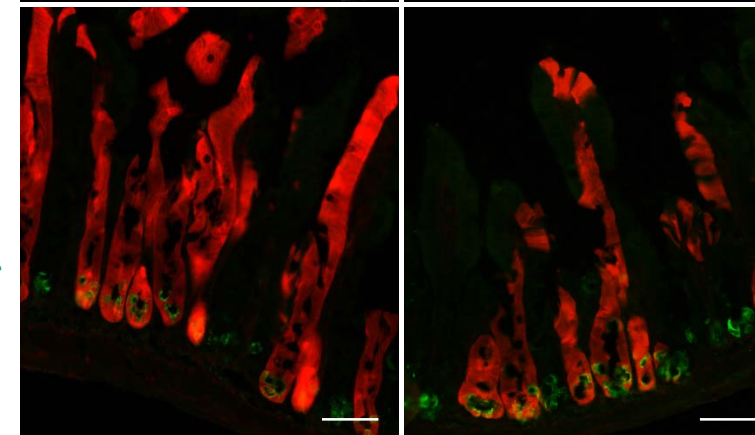


Lgr5^{Cre/+} Lgr5^{Cre/flx}

Plyz



Plyz/RFP



Plyz/RFP/DAPI

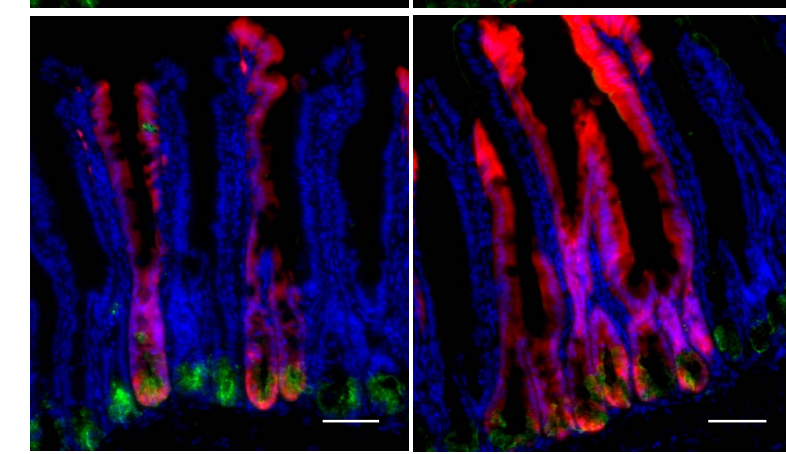
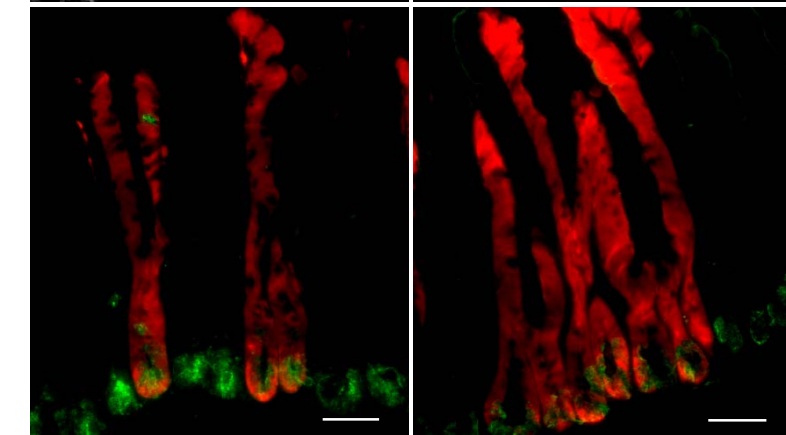
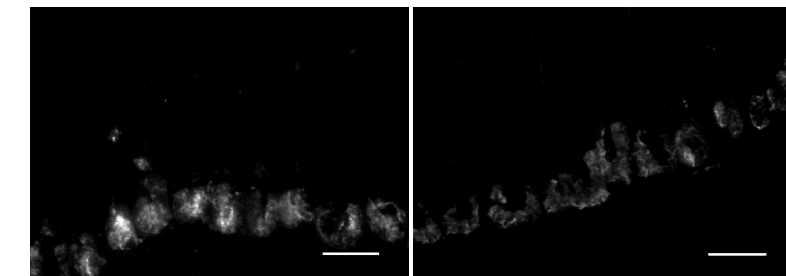
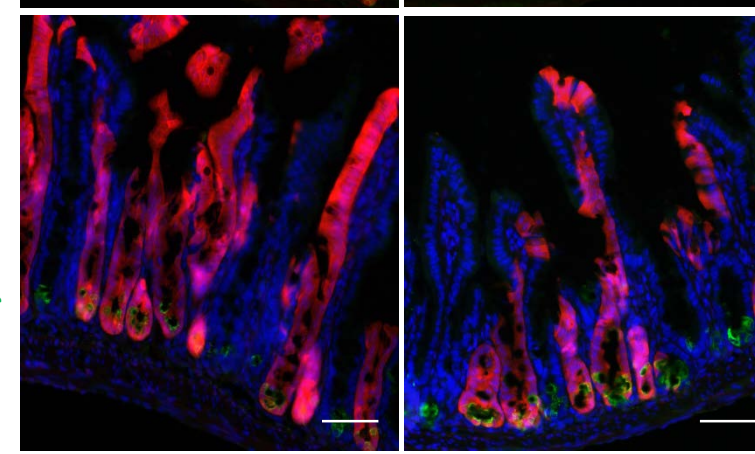
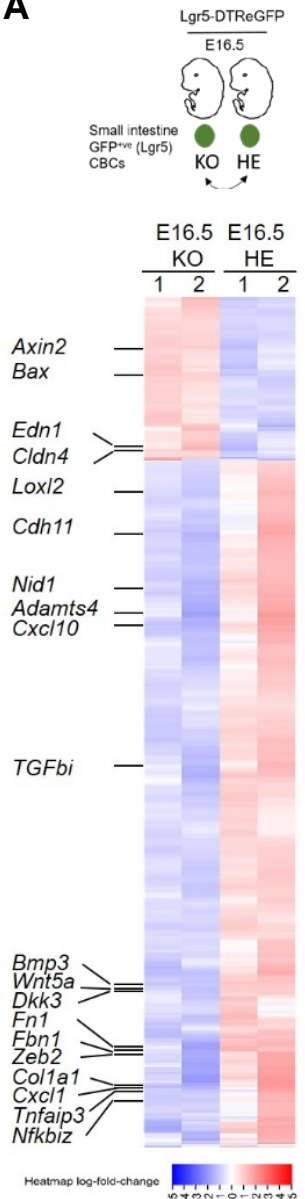
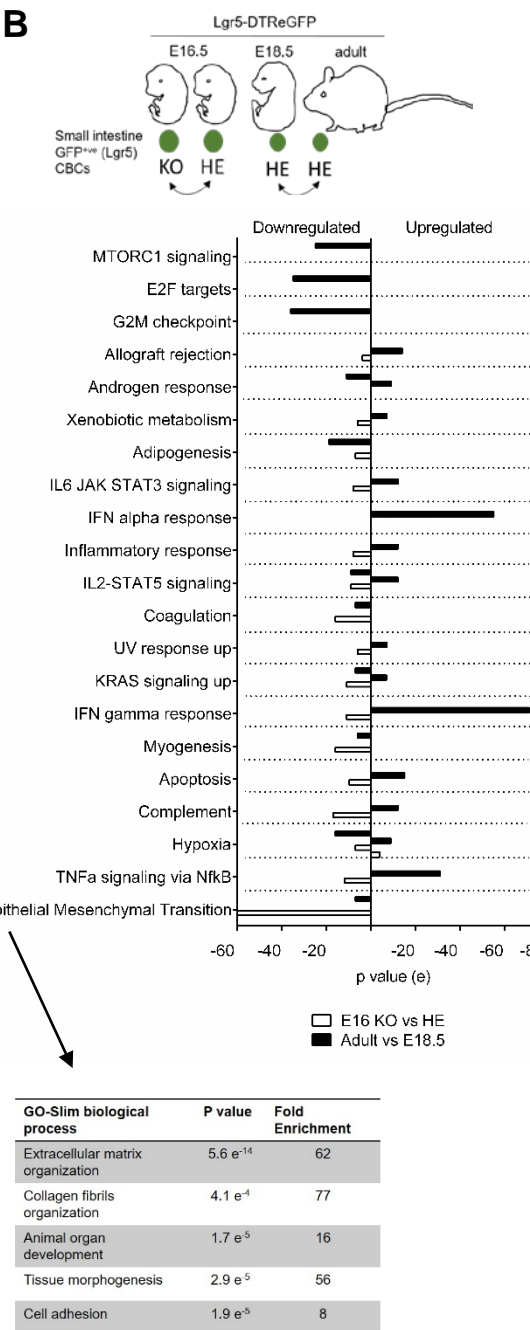


Figure 4

A

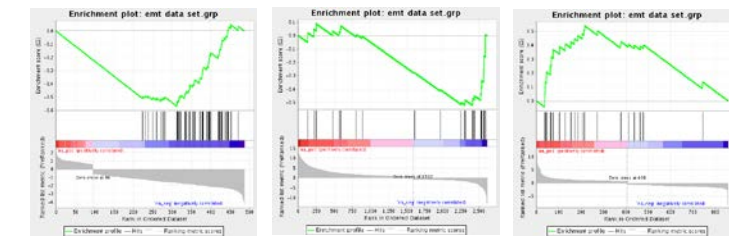


B



C

E16.5 KO/HE vs EMT data set NES -2.39 (pvalue 0.00)
Adult HE/E18.5 HE vs EMT data set NES -1.97 (pvalue 0.005)
Adult KO/Adult HE vs EMT data set NES +1.85 (pvalue 0.01)



E

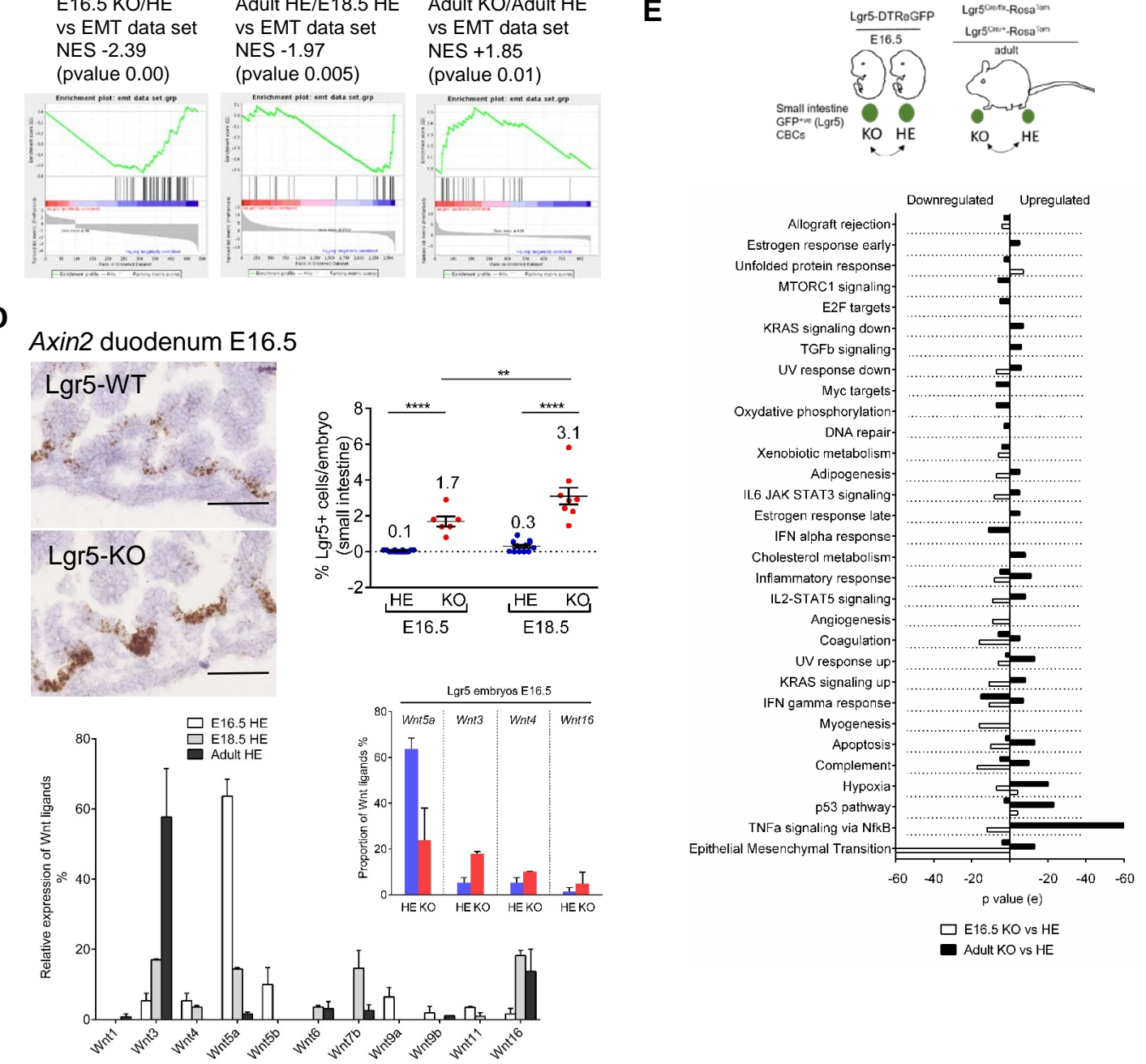
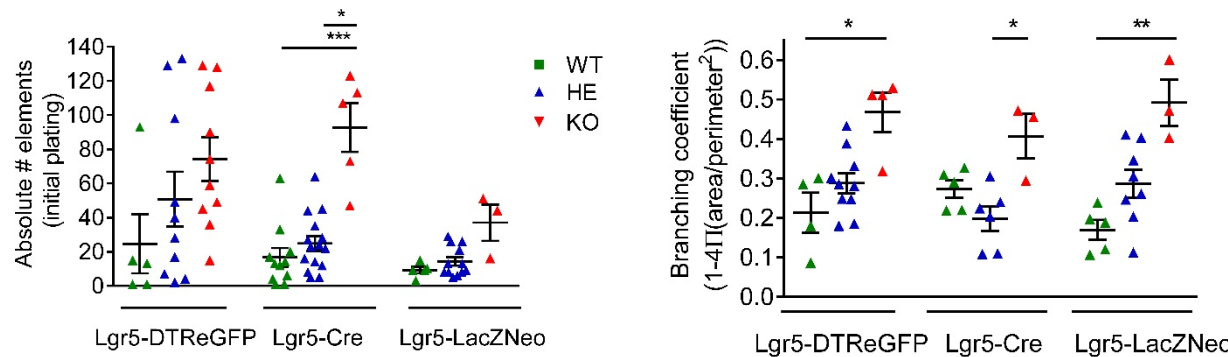
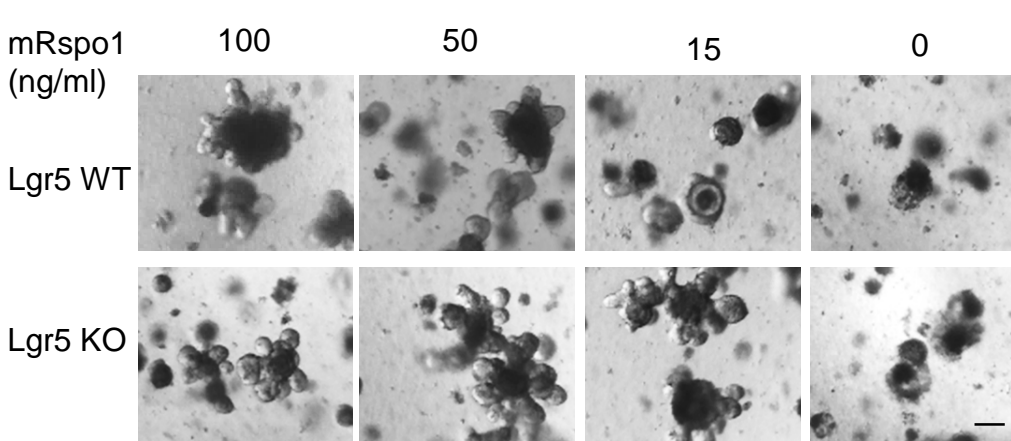


Figure 5

A



B



C

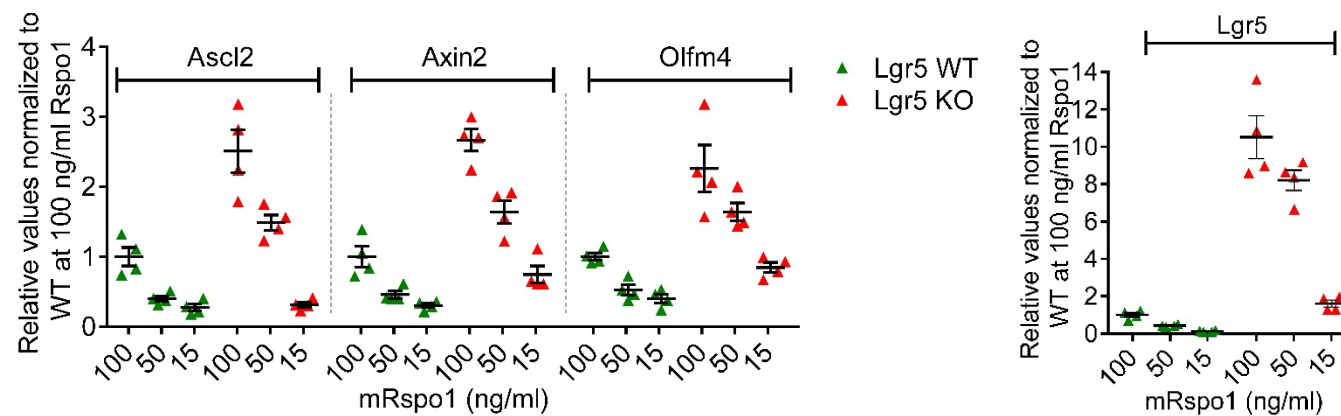
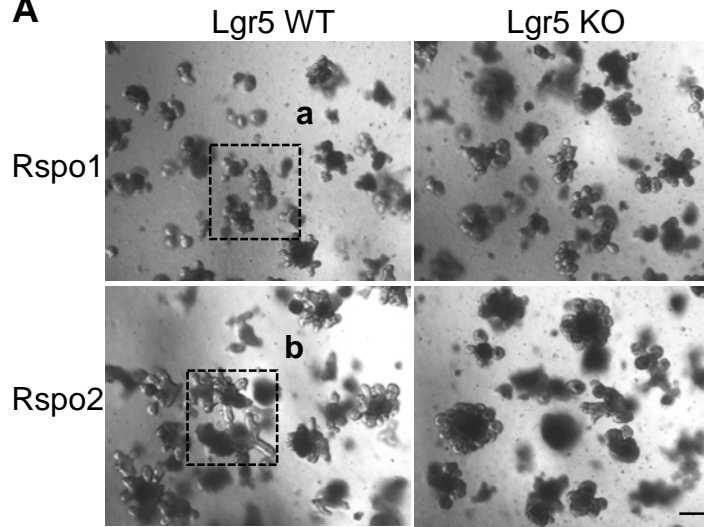


Figure 6

A



Rspo2

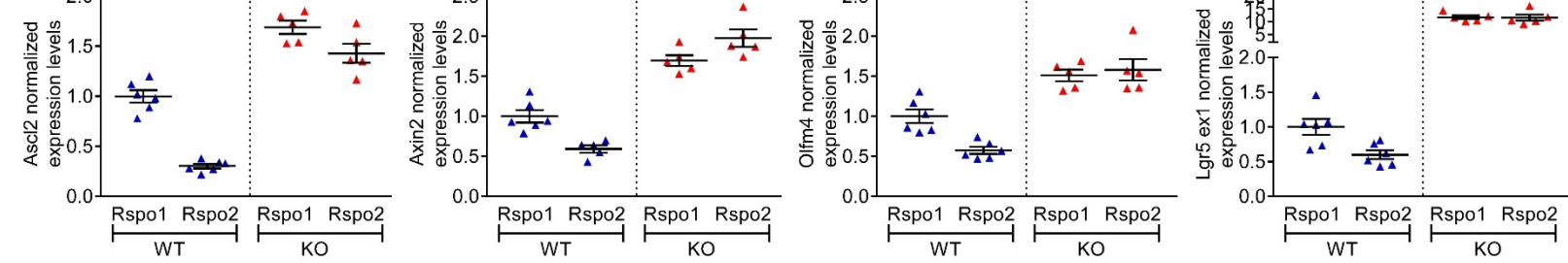
Lgr5 WT

Lgr5 KO

a

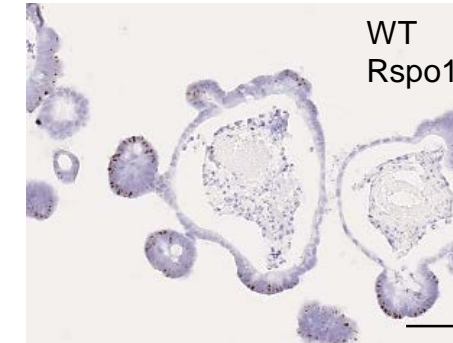
b

B



C

Axin2



WT
Rspo1

WT
Rspo2

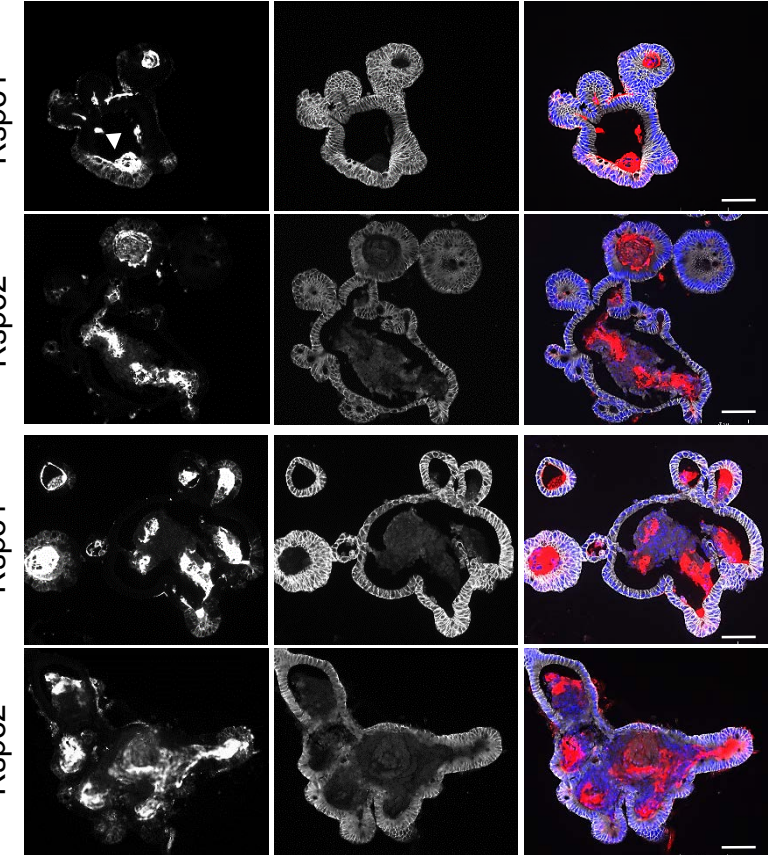
Lgr5 WT

Lgr5 KO

Olfm4

b-catenin

Merge



D

